JMEPEG (2009) 18:21–25
DOI: 10.1007/s11665-008-9262-0

1059-9495/$19.00

FEA of Residual Stress During HVOF Thermal Spraying

J. Stokes and L. Looney

(Submitted May 15, 2008)

Due to the recent advances in thermal spraying technology, considerable research emphasis has been placed on the development of models capable of predicting deposition mechanisms at various stages during the process. In order to gain a deeper knowledge of the mechanisms involved in thermal spraying, it is necessary to isolate the factors affecting these constitutive properties (e.g., residual stress generation) and in doing so quantify the effect of the individual factors. Finite element analysis (FEA) is used in the present research to predict the residual stress generated in a WC-Co deposit produced via the HVOF process. The model is compared to an analytical technique and validated experimentally, the result of which provides a thermo-mechanical modeling procedure with an accuracy greater than 80% of that found experimentally. Combining FEA techniques with analytical and experimental results will enhance the understanding of residual stress in thermal spray techniques.

Keywords finite element analysis, HVOF thermal spraying, residual stress

1. Introduction

It is important to be able to measure the residual stress within a deposit in order to control and reduce its build-up by varying the spray parameters. It has been shown in previous research (Ref 1, 2) that increasing the thickness of the deposit increases the residual stress, promoting fracture or failure of such coatings. Thermal spraying techniques generally produce thin deposits within the micron range; however, it has been shown that higher thicknesses can be achieved with the use of forced cooling (Ref 1-4). Due to the recent advances in thermal spraying technology, considerable research emphasis has been placed on the development of models capable of predicting what happens at various stages during the process. In order to gain a deeper knowledge of the mechanisms involved in thermal spraying, it is necessary to isolate the factors affecting these constitutive properties (e.g., residual stress generation) and in doing so quantify the effect of the individual factors.

Several authors (Ref 5-10) have produced models of the residual stress build-up within the coating structure. In each of these models, the residual stress within the deposit was isolated to the mismatch between the deposit and the substrate. As a result quenching stresses were ignored, therefore differences between the experimental and finite element analysis (FEA) results were expected (Ref 8). The difference between the deposit properties (such as Young's modulus and Poisson's ratio) used in the simulation often differs to the actual properties of the material, thus adding to the differences found between results (Ref 5). This phenomenon is quite complex to predict as, during deposition, quenching stresses generate, while post-deposition cooling stresses generate, hence modeling these two effects poses a lot of problems. The stresses depend on the spraying parameters of the technique used and on the material properties of the coating and substrate. Finite element modeling is a useful tool used to predict an outcome of a particular engineering situation; however, it is only useful if it is validated by experimental results. It is important to remember that numerical techniques will never yield the exact result of an engineering problem, hence the user must always question his/her theoretical results no matter how close they come to the experimental results. The present research introduces a finite element (FE) modeling technique used to predict the residual stress in a deposit (with varying thicknesses and sample size) and the results of which were compared and validated with both analytical and experimental data.

J. Stokes and **L. Looney**, Materials Processing Research Centre & National Centre for Plasma Science and Technology, Dublin City University, Dublin, Ireland. Contact e-mail: joseph.t.stokes@dcu.ie.

2. Residual Stress Determination

In the current study, WC-Co was deposited using the Sulzer Metco DJ HVOF process onto 21 strips (generally 20 mm wide × 80 mm long × 0.075 mm thick) of AISI 316L stainless steel, using a spray distance of 200 mm and a powder feed rate of 38 g/min (the full set of spray parameters are described in Stokes (Ref 2)). The Young's modulus values used in the residual stress equations, for the coating and the substrate, were 185 GPa (found as part of the present study using a cantilever test (Ref 11)) and 200 GPa (Ref 12), respectively. Post deposition, the distributed stresses were deduced by three methods: analytically, experimentally (comparative method), and finally using a proposed FE numerical (thermo-mechanical) model.

2.1 Analytical Method

Residual stress may be calculated analytically using the curvature (by measuring the resulting deflection of the sample) and the physical properties of the sample. Clyne et al. (Ref 13-15) used an analytical method which considers a pair of plates bonded together with a misfit strain $\Delta\varepsilon$ in the x-direction. Results are derived for the top of the deposit, each side of the

deposit/substrate interface and the bottom surface of the substrate. This principle was used to compare the stresses in the deposit attained in the FE model to Clyne's analytical technique.

2.2 Comparative Method

To validate the results found from the analytical method, the experimental results of ten of these samples ranging from a deposit surface compressive stress of 26 MPa to a tensile stress of 82 MPa were selected. Five of these coated samples were polished (plane ground using a P60 SiC abradable grit, working down to a 0.02 μm Nap Cloth) and the residual stress was measured using the Siemens 500 X-ray diffraction system, supported by the Diffrac software. The residual stress was measured for the final five coated samples using the RS-200 Milling Guide (hole-drilling technique) (Ref 1).

2.3 FE Modeling

In this research the ANSYS finite element program was used to predict the residual stress in the coated sample. Modeling of the residual stress was carried out in two ways: one by subjecting the sample to various temperatures until a resulting deflection equalled that found in the experimental results was attained (Fig. 1), labelled as the thermal load system; the second by applying various loads horizontally to the deposit in a tensile manner and similar loads to the substrate in a compressive manner, to generate a moment until a deflection the same as that found experimentally was attained. The choice of tensile or compressive applied to either the deposit/substrate depended on the stress that existed in the experimental sample.

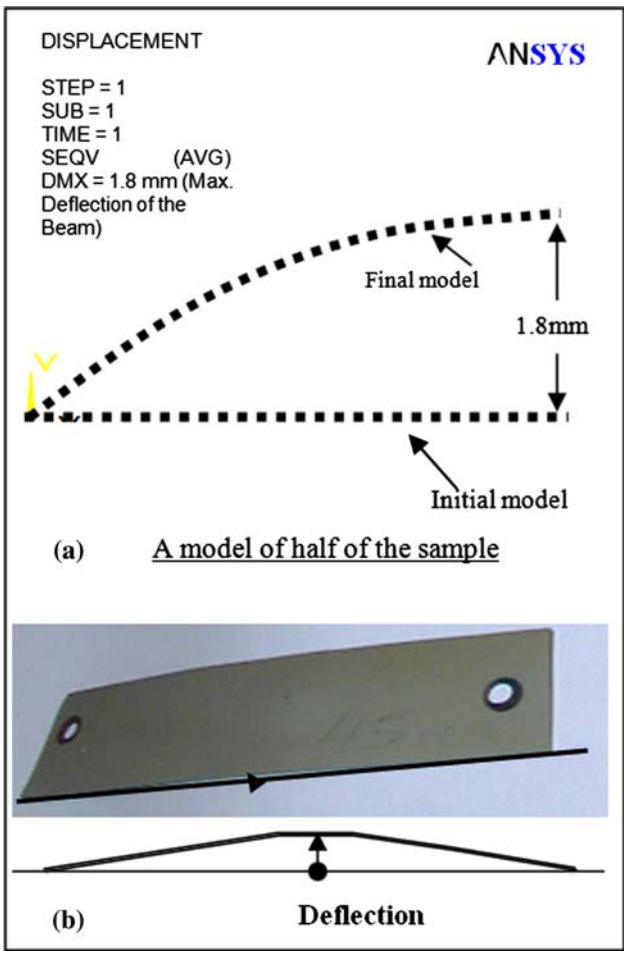

Fig. 1 Resultant deflection for a 0.2-mm deposit on a 0.075-mm substrate: (a) model and (b) deflected sprayed sample

3. Results and Discussion

3.1 Comparison of Analytical and Experimental Results

Previous research has already described the confidence of using Clyne's equations as a measure of distributed residual stress across a deposit, when this technique was compared to X-ray diffraction and hole-drilling experimental techniques (Ref 1). While there were differences in the three measurement methods, correlation between the methods was reasonable, particularly for higher deposit thicknesses. Therefore, the results attained from the analytical results in this research were used to validate the results found using FE modeling.

3.2 Finite Element Model

Initially each modeling system (thermal and generated moment) was compared with the analytical data found for a particular deposited sample. The first modeling test was carried out for a 0.2-mm WC-Co deposit on a 0.075-mm stainless substrate. Various temperatures were applied to the system to yield a deflection of 1.8 mm (resulting deflection found in the experimental data). The stress distribution (at the maximum deflection point) for this sample was measured. Similarly, various loads were applied to the system to yield a deflection of 1.8 mm in the generated moment system and its resulting stress distribution (at the maximum deflection point). In Fig. 2(a), both of these FEA results are compared with the analytical results for a 0.2-mm-thick coating.

As shown in Fig. 2(a), the stress at the top of the deposit in the thermal load system is approximately 60% of that found at the same point in the analytical results. The stress at the top of the deposit in the generated moment system is approximately 80% of that found at the same point in the analytical results. Hence the generated moment finite element result shows the closest result to that found using Clyne's method. The stress change at the interface for the thermal and generated moment systems were −98 and −177 MPa, respectively, compared to −72 MPa found in the experimental data. The thermal system interface stress change is approximately 74% of that found for the same region in the analytical results. Hence the thermal finite element result shows the closest correlation with that found using Clyne's method. The stress at the bottom of the substrate in the generated moment system is approximately 98% of that found at the same point in the analytical results, compared to 25% for the thermal system. Hence in this aspect the generated moment finite element result shows the closest correlation with that found using Clyne's method for this point.

These results suggest that the generated moment finite element results are closest to the analytical results (and therefore the experimental results) for the top and bottom of the sample, whereas the thermal load finite element results are closest to the analytical results (and the experimental results) for the interface region of the sample, based on previous research (Ref 1). This is illustrated in Fig. 2(a). In order to verify if this relationship between experimental data and the

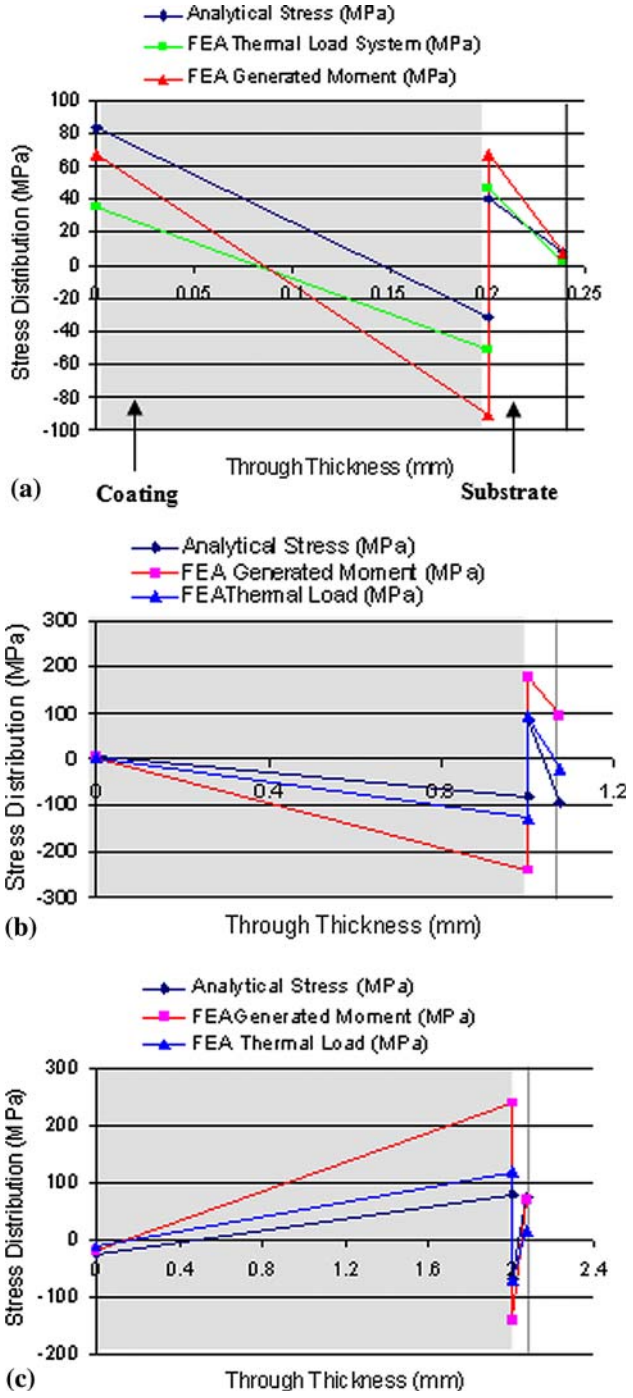

Fig. 2 Finite element and analytical stress analysis of (a) 0.2 mm, (b) 1 mm, and (c) 2 mm thick deposit

two finite element techniques were repeatable, model results were compared to analytical results at higher thicknesses.

The thermal load and generated moment FEA was compared to the analytical data for deposit thicknesses of 1 and 2 mm (Fig. 2b and c). The stress at the top of the 1 and 2 mm deposits in the thermal load system is approximately 62% of that found at the same point in the analytical results. The generated moment system is approximately 82% of that found at the same point in the analytical results. The thermal finite element result shows the closest result for stress change (approximately 75%) to that found using Clyne's method at the interface. The generated moment finite element result shows the closest result (approximately 90%) to that found using Clyne's method for bottom of the sample. Hence the generated moment finite element results are close to the analytical results for the top and bottom of the sample, whereas the thermal load finite element results are close to the results for the interface region of the sample.

The explanation for this is that the generated moment is based on bending theory, hence the deflection of the beam estimates accurately the tensile and compressive stresses at the top and bottom of the sample. This method however does not account for thermal effects and overestimate the stress jump at the interface. The thermal load system accounts for thermal expansion/contraction (misfit strain), hence this model is more successful in predicting the effect this has at the interface. However, the use of the two models would predict quite closely the results found using Clyne's method and what happens during deposition. Therefore, this technique provides a more accurate method of modeling residual stress build-up within deposits as a result of quenching and cooling stress.

It was noted in Stokes (Ref 1) that the deposit surface stress changed from a tensile state to a compressive state at a deposit thickness of 1.2 mm, but after that increased thickness caused the compressive stress to increase further. In order to explain why the thickness increases residual stress, it is necessary to consider the governing phenomena of quenching and cooling stresses. The quenching stress (deposition stress) caused on impact and quenching of individual lamella has been shown to be:

$$\sigma_q \approx \alpha_c(T_m - T_s)E_c \qquad \text{(Eq 1)}$$

There is a possibility of micro-cracking occurring within the deposit during quenching which would release some of the quenching stress; therefore the resultant quenching stress may be less than that given by Eq 1. Equation 2 estimates the stress generated in the coating during cooling after spraying has ceased.

$$\sigma_{cooling} = \frac{[E_c(T_s - T_R)(\alpha_c - \alpha_s)]}{\left[1 + 2\left(\frac{E_c t_c}{E_s t_s}\right)\right]} \qquad \text{(Eq 2)}$$

where α_c, α_s, T_m, T_s, T_R, E_c, E_s, t_s and t_c are the deposit/substrate coefficient of thermal expansion, lamella melting temperature, substrate, and room temperatures and deposit/substrate Young's modulus values and the thicknesses of the deposit/substrate, respectively. The final overall stress at the coating surface can be obtained by adding the quenching stress result to the cooling stress result. When the thickness of the deposit is increased, according to Eq 2 this affects the cooling stresses, which is dependent on the thermal expansion mismatch between the coating and the substrate, thus varies the overall residual stress in the deposit.

3.3 Effect of Substrate Thickness on Residual Stress

In the previous section the substrate thickness remained constant (0.075 mm), this section investigates whether increasing the thickness of the substrate would increase or reduce residual stress. The tests were carried out for a substrate thickness of 1 mm and the results were compared to the results found using a 0.075-mm-thick substrate, for deposits of 1 and 0.2 mm thick. The 0.2-mm deposit thickness results are shown in Table 1.

Analytically, for lower deposit thicknesses (0.2 mm thick), the increase in substrate thickness resulted in a reduction in change in stress from the top of the deposit to the

deposit/substrate interface (from −114 to +100 MPa), changing from compressive to tensile stress. Similarly the tensile stress at the top of the deposit for a low substrate thickness changed from a tensile stress of 82 MPa to a compressive stress of 64 MPa for the 0.2-mm-thick substrate. At higher deposit thicknesses (1 mm thick), the increase in substrate thickness resulted in the stress change from the top of the coating to its interface, from −84 to −65 MPa respectively. The stress at the top of the deposit changed from a tensile stress of 4 MPa to a compressive stress of 1 MPa.

The effect of increasing the substrate thickness has on the residual stress in the deposit is to almost 'invert' the stress distribution, as demonstrated in Fig. 3. This can be explained using the equations for quenching and cooling stresses. The quenching stress for the deposit should be the same for both substrates (0.075 and 1 mm), as the deposit thickness remains constant. Therefore increasing the substrate thickness has the effect of increasing the cooling stress. In this test the substrate thickness is increased by a factor of 13.33, therefore the cooling stress would increase by the same factor. When the quenching and cooling stresses are then combined together (for a substrate thickness of 1 mm), they result in an overall compressive stress at the deposit surface, as opposed to the tensile stress found at this point for a substrate thickness of 0.075 mm. Clyne (Ref 13) states that the analytical curvature of a thermally sprayed sample is related by the following equation:

$$\kappa = \frac{6E_cE_s(h_c + h_s)h_ch_s\Delta\varepsilon}{E_c^2h_c^4 + 4E_cE_sh_c^3h_s + 6E_cE_sh_c^2h_s^2 + 4E_cE_sh_ch_s^3 + E_s^2h_s^4} \quad \text{(Eq 3)}$$

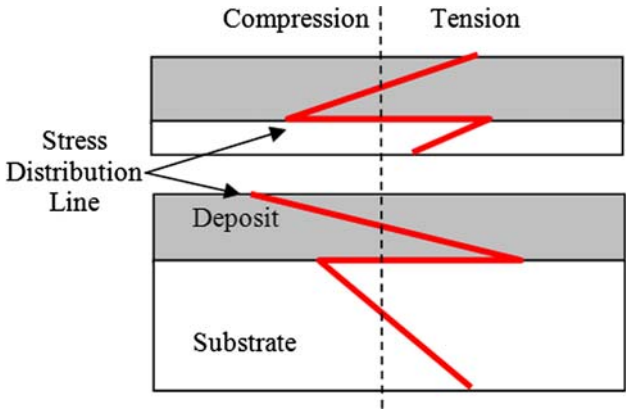

Fig. 3 The effect of substrate thickness on stress

It may be noted that, for a given deposit/substrate thickness ratio (h_c/h_s), the curvature is inversely proportional to the substrate thickness, h_s (Eq 3). Clyne (Ref 13) states that this scale effect is very important in practical terms, since relatively thin substrates are essential if curvatures sufficiently large for accurate measurement are to be generated. Therefore increasing the substrate thickness may reduce the accuracy of the results, but it also has an inverse effect ($\kappa \propto 1/h_s^3$) on the curvature of the sample, turning the sample surface stress from tensile to compressive.

These experimental results were simulated using the two finite element models. Table 1 lists the stresses found at the top of the deposit, both experimentally and numerically (thermal load and structural system). Due to the inaccuracies in the finite element technique, described in the previous section, a difference was observed between the stresses at the top of the deposit. However, both models replicate the effect of increasing the substrate thickness, causing the sample to go from tensile to compressive at the top of the deposit. However, the thermal load system does yield a stress value 58.5% below that of the experimental value. This compares to a stress 18.3% below found using the generated moment system, thus verifying that the latter yields closer values to the experimental results found.

3.4 Effect of Sample Length and Width on Residual Stress

This section investigates whether the size of a thermally sprayed component affected residual stress. Within the size range tested the effect of decreasing the width of the sample is minimal. While it is obvious that similar deposits would result in greater amounts of curvature when sprayed onto longer samples, it is not clear what effect has substrate geometry on stress. In all cases, experimental and analytical tests were carried out for various lengths and widths of sample while keeping the thickness of the deposit (0.2 mm) and the substrate (0.075 mm) constant. Good correlation was found between these results. The length of the sample was varied from 80 mm (used in the last section) to 40 mm, keeping the width of the sample (20 mm) constant. These results were simulated using the two finite element models. Table 2 lists the stresses found at the top of the deposit, both analytically and numerically (thermal load and generated moment). Due to the inaccuracies in the finite element technique, a difference was observed but this was minimal. However, the model replicates the effect of increasing the substrate length. The stress types (tensile/compressive) were maintained; however, the level of stress decreased when shorter sample lengths were used. According to Clyne (Ref 13), the variation of length and width should not

Table 1 The effect of stress on substrate thickness analytically and using the finite element technique

	Analytically		FE model; thermal load and generated moment results combined	
Stress, MPa	Substrate thickness 0.075 mm	Substrate thickness 1 mm	Substrate thickness 0.075 mm	Substrate thickness 1 mm
Top of deposit	+82 MPa	−64 MPa	+80 MPa	−51 MPa
Deposit interface	−32 MPa	+36 MPa	−50 MPa	+40 MPa
Substrate interface	+40 MPa	−35 MPa	+50 MPa	−40 MPa
Bottom of substrate	+8 MPa	+27 MPa	+5 MPa	−6 MPa
Change across deposit	−114 MPa	+100 MPa	−130 MPa	+91 MPa

Note: Positive (+), tensile stress; negative (−), compressive stress

Table 2 The effect of stress on sample length analytically and using the finite element technique

	Analytically		FE model; thermal load and generated moment results combined	
Stress, MPa	**Substrate length 80 mm**	**Substrate length 40 mm**	**Substrate length 80 mm**	**Substrate length 40 mm**
Top of deposit	+82 MPa	+53 MPa	+80 MPa	+50 MPa
Deposit interface	−32 MPa	−21 MPa	−50 MPa	−30 MPa
Substrate interface	+40 MPa	+25 MPa	+50 MPa	+31 MPa
Bottom of substrate	+8 MPa	+5 MPa	+5 MPa	+3 MPa
Change across deposit	−114 MPa	−74 MPa	−130 MPa	−80 MPa

Note: Positive (+), tensile stress; negative (−), compressive stress

result in a variation in stress; however, if the substrate width/length ratio is greater than 0.2, then bifurcation may occur, resulting in a change in stress in the deposit. Hence this phenomenon may explain the stress variation with sample length in the present research.

4. Summary and Conclusion

In this study, the analysis of residual stress generated in high-velocity oxy-fuel thermal spray tungsten carbide-cobalt deposits were analyzed, both analytically and numerical modeling. Previous research carried out by the author showed that Clyne's analytical method produced stress values approximately 30% of that found using the hole drilling and XRD methods, respectively. Hence this technique was used as a benchmark in validating the results of the FE model. The residual stress results found using Clyne's analytical method compared well to the finite element approach introduced in this study. This approach involved combining the results of two models into a thermo-mechanical FE result. The maximum difference found between the analytical and FE results was approximately 14%; however, the FE stress distribution profile matched that found using the analytical technique. This study examined the effect of coating/substrate thickness and sample size, on residual stress in a WC-Co deposit. Increased deposit thickness was found to have the largest effect on stress when compared to initial substrate size. Deposit thickness caused the stress to change from a tensile to a compressive state (Ref 1), but raised the level of stress at higher thicknesses. The thermo-mechanical model introduced in this study provides an innovation method that can be used to determine stress distribution across thermally sprayed deposits, especially in complex systems such as functionally graded deposits, or coatings applied over composite materials, which are not easily analyzed using analytical techniques. The model does not however examine the effect of particle velocity and how this contributes to the stress generated during the process.

References

1. J. Stokes and L. Looney, Residual Stress in HVOF Thermally Sprayed Thick Deposits, *Surf. Coat. Technol.*, 2004, **177–178**, p 18–23
2. J. Stokes and L. Looney, HVOF System Definition to Maximise the Thickness of Formed Components, *Surf. Coat. Technol.*, 2001, **148**(1), p 18–24
3. J. Stokes and L. Looney, *Int. Thermal Spray Conference*, Montréal, Québec, Canada, ASM International, May 8–11, 2000, p 263–271
4. J. Stokes and L. Looney, Properties of WC-Co Components Produced Using the HVOF Thermal Spray Process, *Intern. Conf. on Advances in Materials and Processing Tech*., Dublin, Ireland, August 1999, p 775–784
5. H.D. Steffens and M. Gramlich, FEM-Analysis of Plasma Sprayed Thermal Barrier Coatings, *Int. Thermal Spray Conference*, Orlando, FL, May 25–June 5, 1992, p 531–536
6. X.C. Zhang, B.S. Xu, H.D. Wang, and Y.X. Wu, Modeling of the Residual Stresses in Plasma-Spraying Functionally Graded ZrO_2/NiCoCrAlY Coatings Using Finite Element Method, *Mater. Design*, 2005, **27**(4), p 308–315
7. K.A. Khor and Y.W. Gu, Effects of Residual Stress on the Performance of Plasma Sprayed Functionally Graded ZrO2/NiCoCrAlY Coatings, *Mater. Sci. Eng. A*, 2000, **277**, p 64–76
8. J.K. Wright, J.R. Fincke, R.N. Wright, W.D. Swank, and D.C. Haggard, Experimental and Finite Element Investigation of Residual Stress Resulting from the Thermal Spray Process, *Proceedings of the 8th National Thermal Spray Conference*, Houston, Texas, 1995, p 187–192
9. H. Gruhn, W. Fischer, C. Funke, W. Malliner, and D. Stover, Residual Stress Calculation by Finite Element Methods, *Proceedings of the 9th National Thermal Spray Conference*, Cincinnati, Ohio, 1996, p 869–874
10. H. Gruhn, W. Malliner, and D. Stover, Modeling of Residual Stresses in Plasma Sprayed Multilayer Systems, *Proceedings of the 8th National Thermal Spray Conference*, Houston, Texas, 1995, p 231–236
11. E.F. Rybicki, J.R. Shadley, Y. Xiong, and D.J. Greving, A Cantilever Beam Method for Evaluation of Young's Modulus and Poisson's Ratio of Thermal Spray Coatings, *J. Therm. Spray Technol.*, 1995, **4**(4), p 377–383
12. R.E. Whan, ASM Handbook, *Material Characterization*, American Society for Metals, 9th edn., vol. 10, 1992
13. T.W. Clyne and S.C. Gill, Residual Stresses in Surface Coatings and Their Effects on Interfacial Debonding: A Review of Recent Work, *J. Therm. Spray Technol.*, 1996, **5**(4), p 401–418
14. Y.C. Tsui and T.W. Clyne, An Analytical Model for Predicting Residual Stresses in Progressively Deposited Coatings, Part 1: Planar Geometry, *J. Thin Solid Films*, 1997, **306**, p 23–33
15. T.W. Clyne, Residual Stresses in Surface Coatings and Their Effects on Interfacial Debonding, *Key Eng. Mater.*, 1996, **116–117**, p 307–330